

# Exchanging human Fc $\gamma$ 1 with murine Fc $\gamma$ 2a highly potentiates anti-tumor activity of anti-EpCAM antibody adecatumumab in a syngeneic mouse lung metastasis model

Petra Lutterbuese · Klaus Brischwein · Robert Hofmeister · Sandrine Crommer · Grit Lorenczewski · Laetitia Petersen · Sandra Lippold · Antonio da Silva · Mathias Locher · Patrick A. Baeuerle · Bernd Schlereth

Received: 22 March 2006 / Accepted: 25 July 2006 / Published online: 26 August 2006  
© Springer-Verlag 2006

**Abstract** An important mode of action shared by human IgG1 antibody therapies is antibody-dependent cellular cytotoxicity (ADCC). ADCC relies on the interaction of the antibody's Fc portion with Fc-gamma receptors (Fc $\gamma$ R) on immune effector cells. The anti-tumor activity of human IgG1 antibodies is frequently assessed in mouse models. Binding of human IgG1 to murine Fc $\gamma$ Rs is however of reduced affinity. We here show that ADCC of adecatumumab (MT201), a fully human IgG1 antibody specific for epithelial cell adhesion molecule (EpCAM/CD326), is drastically lower if human peripheral blood mononuclear cells are replaced by murine splenocytes as effector cells. When the variable domains of adecatumumab were genetically fused to a murine IgG2a backbone (yielding mu-adecatumumab), ADCC with murine effector cells was much improved, but at the same time significantly reduced with human effector cells. The serum half-lives of adecatumumab and mu-adecatumumab were determined in mice and dosing schedules established that gave similar serum trough levels during a 4-week antibody treatment. The anti-tumor activities of adecatumumab and mu-adecatumumab were then compared side-by-side in a lung metastasis mouse model established with a syngeneic B16 melanoma line expressing human EpCAM at physiologically relevant levels. Treatment of mice with mu-adecatumumab led to an almost complete prevention of lung metastases,

while the human version of the antibody was much less active. This shows that adecatumumab has high anti-tumor activity when tested in a form that is better compatible with the species' immune system. Moreover, our data suggest to routinely compare in mouse models human IgG1 and murine IgG2a versions of antibodies to properly assess the contribution of ADCC to overall anti-tumor activity.

**Keywords** Adecatumumab · Monoclonal antibody · Fc domain · EpCAM · ADCC · Syngeneic mouse model

## Introduction

During the past decade, chimeric, humanized and human monoclonal antibodies of the IgG1 isotype have been successfully added to the arsenal of anti-cancer therapies. There are currently four registered IgG1 therapies that recognize surface targets on tumor cells and may share antibody-dependent cellular cytotoxicity (ADCC) as a common mode of action. These are anti-CD20 rituximab (Rituxan<sup>®</sup>/MabThera<sup>®</sup>) for treatment of non-Hodgkin lymphoma, anti-HER-2 trastuzumab (Herceptin<sup>®</sup>) for treatment of metastatic breast cancer, anti-EGFR cetuximab (Erbix<sup>®</sup>) for treatment of metastatic colorectal cancer, and anti-CD52 alemtuzumab (Campath<sup>®</sup>) for treatment of refractory chronic lymphatic leukemia. Other registered antibodies in cancer therapy work by different mechanisms, e.g., neutralization of pro-angiogenic VEGF (Avastin<sup>®</sup>), delivery of toxin (Mylotarg<sup>®</sup>) or of radioisotopes (Bexxar<sup>®</sup>, Zevalin<sup>®</sup>). While ADCC was demonstrated for trastuzumab [16, 13], rituximab [9]

P. Lutterbuese · K. Brischwein · R. Hofmeister · S. Crommer · G. Lorenczewski · L. Petersen · S. Lippold · A. da Silva · M. Locher · P. A. Baeuerle (✉) · B. Schlereth  
Micromet AG, Staffelseestr. 2, 81477 Munich, Germany  
e-mail: Patrick.baeuerle@micromet.de

and alemtuzumab [6] and is there considered to be a prime mode of action [10], very little is known about ADCC by cetuximab. Several other IgG1 antibodies, which have been shown to predominantly work by ADCC, are in different stages of clinical development. Examples are the anti-CEA IgG1 labetuzumab [1], anti-carboanhydrase IX IgG1 Rencarex<sup>®</sup> [17] and anti-EpCAM IgG1 adecatumumab [11, 13].

Antibody-dependent cellular cytotoxicity is mediated by a bifunctional binding activity of IgG1. Via its Fc domain, the antibody transiently tethers Fc-gamma receptor (Fc $\gamma$ R)-positive cytotoxic immune cells to antibody-decorated tumor cells. This leads to (i) formation of a cytolytic synapse between cells, (ii) a targeted delivery of cytotoxic proteins, such as perforin and granzymes, by the immune cell and (iii) ultimately induction of apoptosis in tumor cells. Important immune cells participating in ADCC are natural killer (NK) cells bearing the low-affinity Fc $\gamma$  receptor Fc $\gamma$ RIIa (CD16) in humans, and its corresponding receptor Fc $\gamma$ RIII in the mouse. The affinities of these receptors are  $< 1 \times 10^7/M$  for murine Fc $\gamma$ RIII to mouse IgG2a and about  $2 \times 10^7/M$  for human Fc $\gamma$ RIIIA to human IgG1 [18]. The importance of NK cells for ADCC is genetically supported by a correlation of reduced efficacy of rituximab with a polymorphism in CD16 that reduces the receptor's affinity for antibody ligand [2, 4]. A similar correlation was identified for a polymorphism of CD32 [19], suggesting that CD32-positive immune cells also contribute to ADCC although NK cells are major contributors to ADCC when blood cell subpopulations are analyzed [14]. The observation that all IgG1 therapies require high serum trough levels for several months to achieve anti-tumor responses supports that a sustained activation of immune cells is required involving a low-affinity recognition element. In vivo, recruitment of CD16-positive cells by antibody-coated tumor cells is further impeded by high serum concentrations of other IgG1 antibodies that compete for binding [11, 14].

In non-clinical development, the efficacy of novel human IgG1 therapies is frequently assessed in xenotransplant models employing immunodeficient nude mice. Due to the absence of T cells in these mice, many human tumor cell lines are accepted and grow out into measurable tumors. Because nude mice still have NK cells, they are considered to also mediate ADCC by human antibodies. Immunocompetent mouse models employ syngeneic tumor cell lines transfected with the human target antigen. In these models, tumor cells are intravenously injected, get then trapped in lung capillaries and subsequently grow to macroscopically visible lung tumor colonies. A drawback of conventional

mouse models could be that the Fc $\gamma$ 1 domain of human IgG1 antibodies binds with much reduced affinity to mouse Fc $\gamma$ Rs than, for instance, its murine equivalent Fc $\gamma$ 2a. In this case, which requires further analysis, ADCC reactions of human antibodies with murine immune cells are expected to be suboptimal.

Adecatumumab is a fully human IgG1 antibody against EpCAM, which has been shown to act by ADCC and CDC [11]. If the efficacy of a human IgG1 antibody solely relies on ADCC, its anti-tumor activity would be underestimated in conventional mouse models. To test this hypothesis we generated a murine version of adecatumumab by grafting the variable heavy (vH) domain of adecatumumab on a mouse IgG2a domain and fusing the variable light (vL) domain with a mouse c $\kappa$  region. Both antibodies were compared side-by-side with respect to ADCC using human and mouse effector cells. Further, we explored the anti-tumor activity of both antibodies in a lung metastasis model using immunocompetent C57BL/6 mice.

## Materials and methods

### Cell lines

Chinese hamster ovary (CHO) dhfr negative cells were obtained from the German Collection of Microorganisms and Cell Cultures (DSMZ, Braunschweig, Germany) and the KATO III human gastric carcinoma cell line from the European Collection of Cell Cultures (ECACC, Salisbury, UK). CHO dhfr negative cells were grown at 37°C in roller bottles with HyClone culture media (HyClone, Logan, UT, USA) for 7 days before harvest. KATO III cells were cultured in RPMI 1640 media (Invitrogen, Karlsruhe, Germany), supplemented with 10% fetal bovine serum (Invitrogen, Karlsruhe, Germany), at 37°C, in a 5% CO<sub>2</sub> incubator.

The cell line B16F10/EpCAM (clone 3E3), which is stably expressing human EpCAM, was generated at Micromet AG, Munich, Germany. In brief, the parental cell line B16F10 was transfected with the expression vector pEF-ADA-EpCAM and selected with increasing amounts of adenosine/alanosine/uridine and desoxicoformycine. A highly EpCAM-positive clone (3E3) was picked by limiting dilution analysis.

### Construction of mu-adecatumumab

Generation and production of human adecatumumab has been described elsewhere [15]. For the generation of the murine version of adecatumumab, the constant regions were cloned by reverse transcription-PCR

from RNA isolated from OKT3 hybridoma cells expressing a mouse IgG2a antibody directed against human CD3 $\epsilon$ . For the amplification of the cH1–cH3 domains a primer (S IgG2aCH1 + HD69 OH) hybridizing to the 5' end of mouse IgG2a was designed. This primer harbored a stretch of 20 nucleotides complementary to the 3' end of the HD69 vH. The second primer (AS IgG2a *Xba*I) bound to the 3' end of mouse IgG2a sequence including a stop codon and a *Xba*I restriction endonuclease (RE) site. For the amplification of the mouse  $\kappa$  sequence a primer (S IgG $\kappa$  + HD69v $\kappa$ ) was used, which bound to the 5' end of the mouse  $\kappa$  sequence and harbored a 20-nucleotide overhang hybridizing to the adecatumumab vL 3' region. The anti-sense primer (AS mIgG  $\kappa$  *Xho*I) hybridized to the 3' end of mouse  $\kappa$  encoding a stop codon and a *Xho*I RE site. The vH of adecatumumab was amplified from the expression vector pEF-DHFR HC HD69 using the primer S IgG leader hybridizing to the 5' IgG signal peptide and harboring an *Eco*RI RE site and the primer AS HD69vH + IgG2aOH binding to the 3' end of vH HD69 and a having a 20-nucleotide sequence overhang complementary to the 5' mouse IgG2a cH1 sequence. The adecatumumab vL was accordingly amplified with the primers S IgG leader and AS HD69 vL +  $\kappa$  hybridizing to the 3' end of HD69 vL and containing on overhang binding to the 5' end of mouse  $\kappa$ . Finally, heavy and light chain sequences were generated by assembling the corresponding PCR fragments by means of overlapping PCR. For the heavy and light chain, the primer combinations S IgG leader/AS IgG2a *Xba*I and S IgG leader/AS IgG  $\kappa$  *Xho*I were used, respectively. The complete sequence of the mu-adecatumumab HC was then subcloned into the vector pPCR-Script-Cam, the mu-adecatumumab LC sequence was subcloned into pPCR-Script-Amp. The correct sequence was verified by automated DNA sequencing. Finally, the HD69 chimeric heavy chain was cloned into the expression vector pEF-DHFR, which was digested with *Eco*RI and *Xba*I. The light chain digested with *Eco*RI and *Xho*I was inserted into pEF-ADA, which was cut with *Eco*RI/*Sal*I. Mu-adecatumumab was produced in CHO dhfr-cells transfected with the expression vectors pEF-DHFR-HD69 HC and pEF-ADA-HD69 LC and mu-adecatumumab purified from cell culture supernatants in a one step process using a Protein G column and Äkta FPLC System (Amersham Biosciences, Little Chalfont, UK).

The human IgG1 kappa control antibody (I-5154) was obtained from Sigma-Aldrich (Taufkirchen, Germany) and served as isotype control for adecatumumab. The murine IgG2a antibody Orthoclone

OKT3 (Janssen-Cilag, Neuss, Germany) served as an isotype control for mu-adecatumumab.

#### Binding comparison of adecatumumab and mu-adecatumumab

Kinetic binding experiments with adecatumumab and mu-adecatumumab were performed using surface plasmon resonance on the BIAcore™ 2000 (BIAcore AB, Uppsala, Sweden) with a flow rate of 5  $\mu$ l/min and HBS-EP (0.01 M HEPES, pH 7.4, 0.15 M NaCl, 3 mM EDTA, 0.005% surfactant P20) as running buffer, at 25°C. The extracellular domain of the EpCAM antigen (residues 17–265) was immobilized on a CM5 sensor chip with different densities for each flow cell.

Binding kinetics of the antibodies were measured by injecting 10  $\mu$ l of protein solution at concentrations ranging from 2 to 0.07  $\mu$ M and monitoring the dissociation for 100 s. The data were fitted using BIAevaluation™ software determining the rate constant for dissociation and association kinetics. From the rate constants the equilibrium binding constant  $K_D$  was calculated.

For the competition binding experiments, the binding of a single concentration of one antibody (ligand) was measured in the presence of various concentrations of the competitor antibody. In order to reach equilibrium binding, B16/EpCAM 3E3 cells (100,000/well) were incubated for 18 h at room temperature in 150  $\mu$ l of FACS buffer (PBS, 1% FCS, 0.05% NaN<sub>3</sub>) containing the respective ligand and competitor antibody. For detection of the binding of the ligand antibody, a FITC-labeled detection antibody specific for human or mouse antibodies was used (anti-human IgG-FITC, ICN 67217; anti-mouse IgG-FITC, Sigma F-6257). Assay data were analyzed with Prism software (GraphPad Software Inc., San Diego, CA, USA). After non-linear regression of the competitive binding curves the  $K_i$  value for the competitor could be calculated knowing the  $K_D$  value from a parallel saturation binding experiment.

#### Bioactivity comparison of adecatumumab and mu-adecatumumab

For ADCC assays, murine NK cells were prepared by negative selection of C57BL/6 splenocytes using the murine NK cell isolation kit from BD Biosciences (San Jose, CA, USA) as described by the manufacturer. Isolated NK cells were cultured for 7–14 days in RPMI 1640/10% FCS supplemented with 1,700 U/ml Proleukin (Chiron GmbH, Munich, Germany) at a density of about  $1 \times 10^6$  cells/ml. Every 2–3 days, cells were

counted and fresh medium added. After 7–14 days in culture, NK cell purity was between 90 and 100%. Stimulated murine NK cells were re-suspended in RPMI 1640/10% FCS at a concentration of  $1.6 \times 10^7$  cells/ml and used as effector cells in ADCC assays. For the preparation of human effector cells, peripheral blood mononuclear cells (PBMC) were enriched by Ficoll-Hypaque gradient centrifugation [11], washed and re-suspended at  $1.2 \times 10^7$  cells/ml.

EpCAM-positive Kato III cells were used as target cells and labeled with the fluorescent membrane dye PKH-26 (Sigma, Taufkirchen, Germany) according to the manufacturer's protocol in order to distinguish target from effector cells in subsequent FACS analysis. PKH-26 labeled target cells were adjusted to a density of  $4 \times 10^5$  and  $6 \times 10^5$  cells/ml for assays with murine and human effector cells, respectively. Equal volumes of target and effector cell suspensions were mixed resulting in an effector-to-target (E:T) ratio of approximately 50:1 and 20:1 for murine and human effector cells, respectively, and 50  $\mu$ l added/well of a 96-well U-bottom microtiter plate (Greiner, Solingen, Germany). Fourfold serial dilutions of adecatumumab and tenfold serial dilutions of mu-adecatumumab were prepared and 50  $\mu$ l added/well resulting in a concentration range of 50,000–0.05 ng/ml for adecatumumab and 50,000–0.2 ng/ml for mu-adecatumumab. ADCC reactions were incubated for 10 and 4 h at 37°C for assays with murine and human effector cells, respectively. Propidium iodide (PI) was added to a final concentration of 1  $\mu$ g/ml and  $5 \times 10^4$  cells analyzed by flow cytometry using a FACSCalibur instrument (Becton Dickinson, Heidelberg, Germany). Dose–response curves were computed by non-linear regression analysis using a four-parameter fit model provided with the GraphPad Prism software (GraphPad Software). All experiments were performed in triplicates.

Quantification of cytotoxicity was based on the number of dead target cells in relation to the total number of target cells in each test sample. The specific cytotoxicity was calculated by the formula: (dead target cells (sample)/total target cells (sample))  $\times$  100.

#### Animal studies

In vivo experiments were performed in female 6–10 week old immunocompetent C57BL/6 mice bred at the Institute of Immunology (Munich University, Germany). The mice were maintained under sterile and standardized environmental conditions ( $20 \pm 1^\circ\text{C}$  room temperature,  $50 \pm 10\%$  relative humidity, and 12-h light/dark rhythm) and received autoclaved food and bedding (ssniff, Soest, Germany) as well as drinking

water ad libitum. All experiments were performed according to the German Animal Protection Law with permission from the responsible local authorities.

Statistical analysis of the mean number of lung tumor colonies of the corresponding treatment groups versus the vehicle control group was performed using the Student's *t*-test.

#### Pharmacokinetic analysis

To generate a pharmacokinetic profile of adecatumumab and mu-adecatumumab, 20 female C57BL/6 mice were intravenously injected with 300  $\mu$ g of the respective antibody and animals allocated to four different groups of 5 mice each. Different groups were alternately bled at different time points after injection (pre-dose, 0.5, 1, 2, 4 and 10 h, 1, 2, 4, 7, 9, 11, 14, 17, 21, 24 and 28 days) and serum concentrations quantified by specific ELISAs.

ELISA plates (NUNC, Wiesbaden, Germany) were coated with 100  $\mu$ l (5  $\mu$ g/ml) of rat anti-adecatumumab antibody (Micromet AG, Munich, Germany). Plates were incubated overnight at 4°C and blocked with PBS/1% bovine serum albumin for 60 min at 25°C. Test samples were diluted in PBS/10% mouse plasma pool, 100  $\mu$ l added/well and incubated for 60 min at 25°C. For adecatumumab quantification, plates were incubated with 100  $\mu$ l (0.15  $\mu$ g/ml) of chicken anti-adecatumumab antibody conjugated with biotin (Micromet AG) at a final concentration of 2  $\mu$ g/ml for 60 min at 25°C followed by incubation for 60 min at 25°C with 100  $\mu$ l streptavidin conjugated with alkaline phosphatase (Dako, Hamburg, Germany) at a final concentration of 0.5  $\mu$ g/ml. For mu-adecatumumab quantification, plates were incubated with 100  $\mu$ l of goat anti-mouse antibody conjugated with alkaline phosphatase (Sigma, Taufkirchen, Germany) for 60 min at 25°C. Finally, plates were incubated with 100  $\mu$ l of substrate (1 mg/ml of *p*-NPP dissolved in 0.2 M TRIS buffer; Sigma, Taufkirchen, Germany) for 20 min at 25°C and the absorbance (405 nm) read on Power WaveX select (Bio-Tek instruments, Bad Friedrichshall, Germany). Twofold serial dilutions of each test sample were analyzed in duplicates and OD values that were within the linear range of the standard curve were used to calculate the concentration of adecatumumab and mu-adecatumumab.

Pharmacokinetic calculations of adecatumumab and mu-adecatumumab were performed by the pharmacokinetic software package WinNonlin Professional 4.1 (Pharsight Corporation, Mountain View, CA, USA; 2003). Parameters were determined by non-compartmental analysis (NCA). The NCA was based on model 201 (intravenous bolus injection).

## Tumor model

B16/EpCAM cells ( $1 \times 10^5$ ) were intravenously injected into C57BL/6 mice and animals treated three times a week with the indicated dose levels of adecatumumab, mu-adecatumumab or human IgG1 control antibody starting 1 h after B16/EpCAM inoculation. Mice were sacrificed and dissected on day 26 after B16/EpCAM cell injection. Lungs were filled with tissue teck (Vogel GmbH, Giessen, Germany) and analyzed macroscopically for the number of tumor colonies. To monitor exposure to the respective antibodies three animals per group were alternatingly bleed before and 30 min after the 3rd, 6th, 9th, 11th infusion as well as at the end of the study.

## Results

### Generation of mu-adecatumumab

The murine IgG2a version of adecatumumab (mu-adecatumumab) was generated by combining the vL and vH regions of adecatumumab (formerly HD69) [15] with the mouse constant  $\kappa$  light and constant  $\text{cH1-cH3}$  heavy region sequences, respectively. The mouse constant domains were amplified from mRNA isolated from the human CD3 $\epsilon$ -specific hybridoma OKT3. By this means, mu-adecatumumab retained the variable regions of adecatumumab required for human EpCAM binding and acquired the Fc portion of murine IgG2a. Expression vectors encoding heavy and light chains of mu-adecatumumab were stably transfected into CHO dhfr negative cells and secreted mu-adecatumumab was purified from cell culture supernatants by Protein G affinity chromatography. SDS/PAGE and Western blot analysis indicated a purity > 95% for mu-adecatumumab. The concentration of the antibody in CHO cell culture supernatant was approximately 11 mg/l.

### Adecatumumab and mu-adecatumumab show comparable EpCAM binding affinity and specificity

Plasmon resonance spectroscopy and binding competition analysis demonstrated that mu-adecatumumab retained binding affinity and specificity comparable to that of the parental human IgG1 antibody adecatumumab. Binding curves to recombinant EpCAM coated on BIAcore sensor chips were recorded at four concentrations of adecatumumab and mu-adecatumumab in five independent experiments. The equilibrium dissociation constant ( $K_D$ ) for EpCAM binding was determined with  $66.6 \pm 33.6$  and  $90.9 \pm 36.4$  nM

for adecatumumab and mu-adecatumumab, respectively. Differences in  $K_D$  values were not statistically different indicating that affinity for EpCAM was retained in mu-adecatumumab. To determine whether mu-adecatumumab had retained the epitope specificity of adecatumumab, EpCAM-expressing B16/EpCAM 3E3 murine melanoma cells were incubated with a non-saturating concentration of mu-adecatumumab (4  $\mu\text{g/ml}$ ). In competition binding analyses, increasing concentrations of adecatumumab or a human IgG1 isotype control antibody were tested for displacement of the bound antibody. As determined by flow cytometry, adecatumumab effectively competed with mu-adecatumumab for binding to B16/EpCAM 3E3 cells while the isotype control antibody had no effect (Fig. 1).

### Adecatumumab and mu-adecatumumab show strong species-specific differences in ADCC

We studied the cytotoxic potency of adecatumumab and mu-adecatumumab in ADCC assays using human and murine effector cells. The human gastric carcinoma cell line KATO III with approximately  $1.3 \times 10^6$  EpCAM binding sites per cell was employed as target. Adecatumumab showed a much higher ADCC activity than mu-adecatumumab when unstimulated human PBMC were used as effector cells (Fig. 2a). Half-maximal lysis ( $\text{EC}_{50}$ ) was seen at a concentration of 169.6 ng/ml for adecatumumab versus 2,110 ng/ml for mu-adecatumumab, resulting in a 12.4-fold potency difference. None of the antibodies exerted ADCC

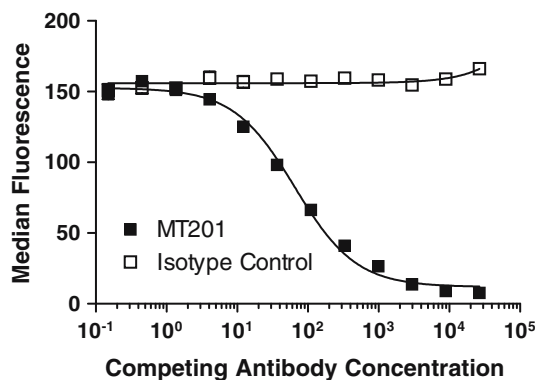


**Fig. 1** Competition by adecatumumab of mu-adecatumumab binding to B16/EpCAM 3E3 cells. B16/EpCAM 3E3 murine melanoma cells were incubated with 4  $\mu\text{g/ml}$  of mu-adecatumumab followed by binding competition with increasing concentrations of either human adecatumumab (*dark square*) or human IgG1 isotype control antibody (*open square*). Mu-adecatumumab bound to B16/EpCAM 3E3 cells was determined by flow cytometry using a fluorescently labeled anti-mouse IgG antibody, and data analyzed with Prism software (GraphPad Software Inc.)

activity when tested in assays with unstimulated mouse splenocytes or NK cells isolated thereof (data not shown), which is consistent with published work [12]. However, when NK cells pre-stimulated with IL-2 were used at an E:T ratio of 50:1, adecatumumab showed a dose-dependent ADCC activity. Mu-adecatumumab was found to be more efficacious with murine NK cells than adecatumumab (Fig. 2b). The murine version of adecatumumab induced half-maximal target cell lysis at a concentration of 38.1 ng/ml and human adecatumumab at 1,664 ng/ml, resulting in 43.7-fold higher potency for mu-adecatumumab with

murine cells. Human IgG1 and murine IgG2a isotype control antibodies did not elicit specific ADCC activity under either experimental condition underscoring target specificity of the antibodies.

#### Pharmacokinetic properties of adecatumumab and mu-adecatumumab in mice

Single administration of 300  $\mu$ g adecatumumab and mu-adecatumumab resulted in maximum serum concentrations ( $C_{max}$ ) of 119.2 and 204  $\mu$ g/ml, respectively, 30 min after i.v. bolus injection into C57BL/6 mice. Serum concentrations of the antibodies were well detectable until the end of the 28-day study period (Fig. 3). Serum concentration versus time profiles for both adecatumumab and mu-adecatumumab exhibited a bi-exponential curve progression with an early distribution phase between 0 and 10 h and a terminal elimination phase. Despite curve progression looking similar for both antibodies, mu-adecatumumab doses resulted in constantly higher serum concentration compared to adecatumumab, which was also reflected by higher exposure ( $AUC_{last}$ ) values of 519.8 days $\cdot$  $\mu$ g/ml for mu-adecatumumab versus 335.9 days $\cdot$  $\mu$ g/ml for adecatumumab, respectively. The volume of distribution ( $V_z$ ) and the clearance (CL) were calculated with 5.28 ml and 0.56 ml/day for mu-adecatumumab, and with 7.78 ml and 0.86 ml/day for adecatumumab. Both, the volume of distribution and the clearance were higher for adecatumumab compared to mu-adecatumumab. The elimination rate constants resulted in similar distribution half-lives ( $T_{1/2-\alpha}$ ) of 0.27 and 0.31 days and terminal elimination half-lives ( $T_{1/2-\beta}$ )

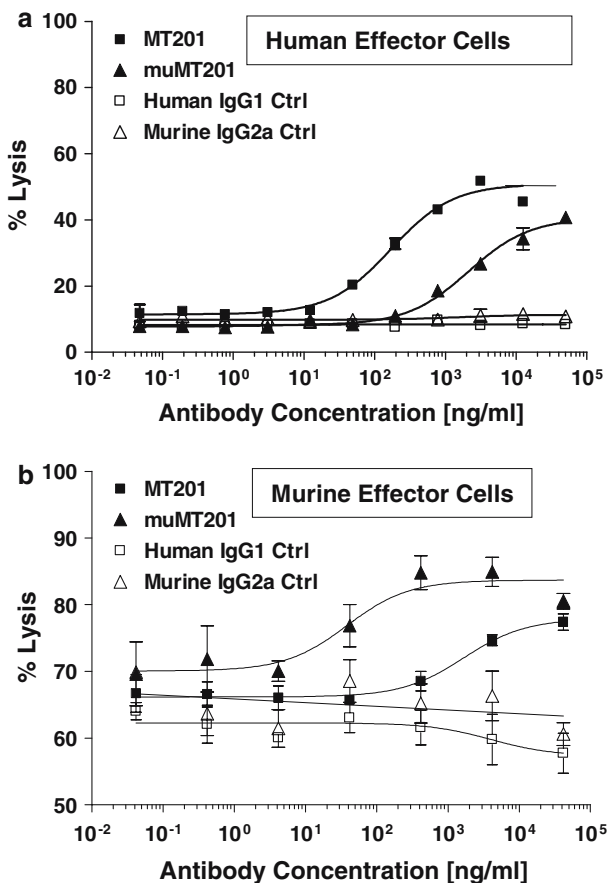


**Fig. 2** ADCC of mu-adecatumumab and adecatumumab with human and murine effector cells. **a** Kato III cells and non-stimulated human PBMC were co-incubated at a ratio of 1:20 in the presence of indicated adecatumumab (filled squares) and mu-adecatumumab (filled triangles) concentrations. Human IgG1 (open squares) and mouse IgG2a (open triangles) isotype control antibodies served as negative controls. ADCC activity was measured after 4 h. Target cell lysis was determined by PI uptake using flow cytometry. **b** Kato III cells and IL-2 pre-stimulated murine NK cells were co-incubated at a ratio of 1:50 in the presence of indicated adecatumumab (filled squares) and mu-adecatumumab (filled triangles) concentrations. Human IgG1 (open squares) and mouse IgG2a (open triangles) isotype control antibodies were used as negative controls. ADCC activity was measured after 10 h. Error bars show standard deviations of triplicate wells

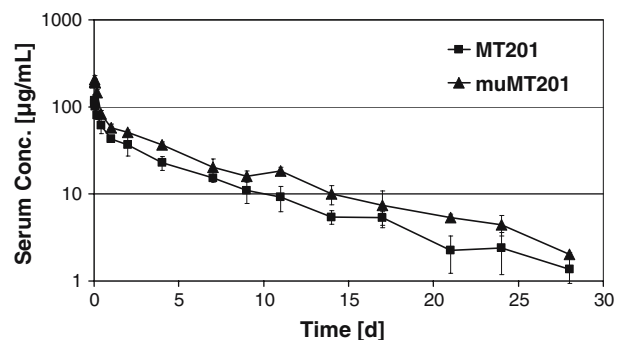


**Fig. 3** Pharmacokinetics of adecatumumab and mu-adecatumumab following i.v. bolus injection in C57BL/6 mice. Twenty female C57BL/6 mice were intravenously injected with 300  $\mu$ g of adecatumumab or mu-adecatumumab and animals allocated to four different groups of five mice each. Different groups were alternately bled at different time points after injection (pre-dose, 0.5, 1, 2, 4 and 10 h, 1, 2, 4, 7, 9, 11, 14, 17, 21, 24 and 28 days) and serum concentrations of the respective antibodies quantified by specific ELISAs. Error bars show standard deviations from five different animals per group

of 6.21 and 6.57 days for adecatumumab and mu-adecatumumab, respectively.

#### Establishment of a syngeneic lung metastasis model in C57BL/6 mice

The *in vivo* efficacy of adecatumumab and mu-adecatumumab was compared side-by-side in an immunocompetent C57BL/6 mouse model. We established a tumor model with B16 mouse melanoma cells in which, following intravenous injection, tumor cell colonies are formed in the lungs. In order to render B16F10 cells amenable for immunotherapy with human EpCAM-specific antibodies, cells were stably transfected with an expression vector encoding human EpCAM. Subclone B16/EpCAM 3E3 was selected and its EpCAM expression determined by saturation binding. Approximately  $2.0 \times 10^6$  EpCAM binding sites were measured, a number which is comparable to the  $1.3 \times 10^6$  EpCAM sites expressed on KATO III human gastric carcinoma cells. The high-level of EpCAM expression on B16/EpCAM cell was found to be stable for at least 6 weeks in cell culture even in the absence of selection pressure (data not shown).

For establishment of the animal model, syngeneic B16/EpCAM cells were intravenously injected at different numbers into C57BL/6 mice and the number of tumor colonies in lung tissue counted at different time points after inoculation. Conditions under which  $1 \times 10^5$  injected B16/EpCAM cells resulted in an average of 80–100 tumor colonies between 21 and 28 days after injection were chosen for the following efficacy studies.

#### Superior anti-tumor activity of mu-adecatumumab in immunocompetent mice

The single-dose pharmacokinetic profiles of adecatumumab and mu-adecatumumab were used for modeling a dosing regimen that would result in serum trough levels at or above 30  $\mu\text{g}/\text{ml}$ . This concentration corresponds to the targeted trough levels for adecatumumab in two ongoing clinical phase II studies. Based on PK modeling, a loading dose of 600  $\mu\text{g}/\text{mouse}$  followed by maintenance doses of 250  $\mu\text{g}/\text{mouse}$  three times per week were selected for adecatumumab and for the human IgG control antibody. For mu-adecatumumab, a loading dose of 300  $\mu\text{g}/\text{mouse}$  and maintenance doses of 125  $\mu\text{g}/\text{mouse}$  three times per week were administered. Following intravenous inoculation with  $1 \times 10^5$  B16/EpCAM, ten animals per group were treated with the antibodies and serum levels of adecatumumab (Fig. 4a) and mu-adecatumumab (Fig. 4b)

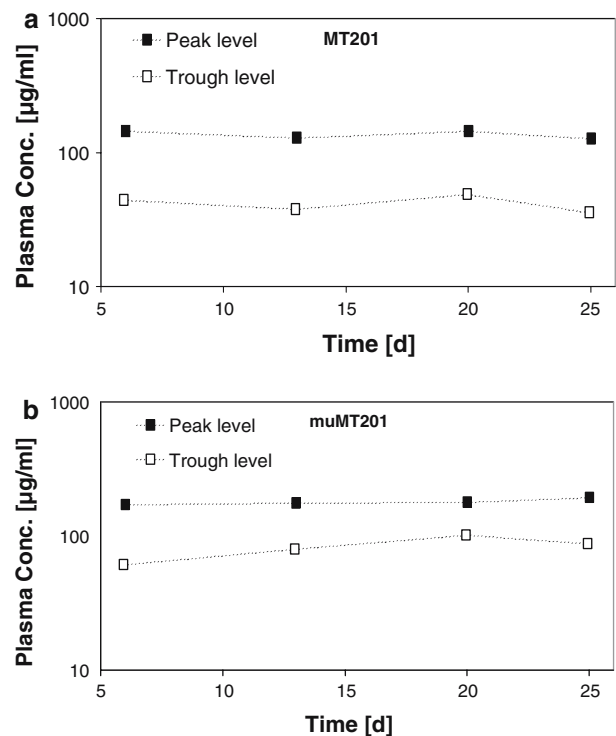


**Fig. 4** Adecatumumab and mu-adecatumumab peak to trough levels following repetitive intravenous treatment of C57BL/6 mice. Ten C57BL/6 mice were intravenously injected with adecatumumab, mu-adecatumumab and human IgG isotype control three times a week for four consecutive weeks. A single loading dose of 600  $\mu\text{g}/\text{mouse}$  followed by maintenance doses of 250  $\mu\text{g}/\text{mouse}$  were selected for adecatumumab and for the human IgG control antibody. For mu-adecatumumab, a loading dose of 300  $\mu\text{g}/\text{mouse}$  and maintenance doses of 125  $\mu\text{g}/\text{mouse}$  were administered. For monitoring peak (*filled squares*) and trough plasma concentrations of adecatumumab and mu-adecatumumab (*open squares*), three animals per group were alternately bled before and 30 min after the 3rd, 6th, 9th, 11th infusion as well as at the end of the study. Antibody concentrations were determined by specific ELISAs

determined after the 3rd, 6th, 9th and 11th administration. Adecatumumab injections resulted in mean peak to trough plasma concentrations of 136–41  $\mu\text{g}/\text{ml}$ , which were close to the expected plasma concentrations of 150–30  $\mu\text{g}/\text{ml}$  during the course of the study. Mean peak to trough concentration of mu-adecatumumab were determined with 172–82  $\mu\text{g}/\text{ml}$ . Although plasma concentrations of mu-adecatumumab were somewhat higher than for adecatumumab, the overall exposure with both antibodies was considered to be in an effective and comparable range.

Macroscopic inspection of mouse lungs showed that both, the human and murine version of the anti-EpCAM antibody, led to a strong reduction of tumor growth compared to the isotype control (Fig. 5a, b). While lungs from mice treated with mu-adecatumumab

had very few detectable tumors (Fig. 5a, bottom panels), small tumors were still visible on lungs from mice treated with human adecatumumab (Fig 5a, middle panels). Although the size of tumor colonies in human adecatumumab-treated mice was smaller than tumor size in lungs of animals treated with the human isotype control antibody (Fig. 5a), the number of colonies was only slightly reduced after adecatumumab treatment without reaching statistical significance (Fig. 5b). In contrast, treatment with mu-adecatumumab induced a highly significant reduction in the number of lung tumor colonies by > 85% ( $P < 0.0001$ ), and the few remaining tumor colonies were of very small size (Fig. 5a, b).

## Discussion

This study shows that the species origin of the Fc portion of a monoclonal antibody can greatly influence

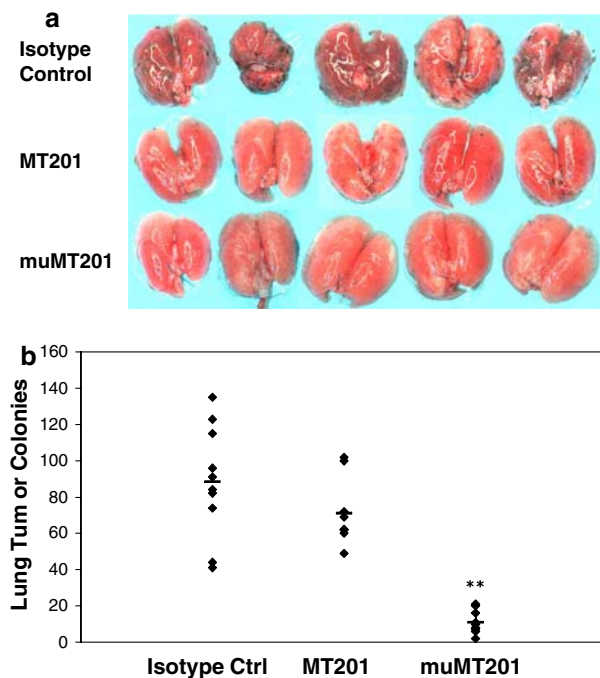


**Fig. 5** The effect of mu-adecatumumab and adecatumumab on lung tumor colony formation in immunocompetent mice. B16/EpCAM cells ( $1 \times 10^5$ ) were intravenously injected into C57BL/6 mice and animals treated three times a week with the indicated doses of adecatumumab, mu-adecatumumab or human IgG1 control antibody starting 1 h after intravenous B16/EpCAM cell injection. Mice were sacrificed on day 26 after B16/EpCAM cell injection. **a** Lungs were filled with tissue teck and digital photographs taken. **b** The number of lung tumor colonies was determined macroscopically. While *symbols* indicate the number of lung colonies for one single mouse, the *black bar* indicates means of each group. *Asterisks* indicate statistical differences between treatment and isotype control group (\*\* $P \leq 0.01$  as determined with Student's *t*-test)

anti-tumor activity in a mouse model. The increased anti-tumor activity of murine Fc $\gamma$ 2a versus human Fc $\gamma$ 1 in a fully immunocompetent mouse model appears to be primarily based on enhanced ADCC. This is evident from ADCC assays where the version of adecatumumab with a murine Fc $\gamma$ 2a portion was much more cytotoxic against cancer cells than the human IgG1 version when murine effector cells were used. CDC is unlikely to significantly contribute to the species dependency of anti-tumor activity. Human adecatumumab and murine edrecolomab, two antibodies binding with similar affinity to human EpCAM, showed identical CDC with human complement [11]. Moreover, knock-out of the common  $\gamma$  signaling chain of Fc $\gamma$ Rs did almost completely neutralize the anti-tumor activities of trastuzumab and rituximab in a mouse xenotransplant model, suggesting a small contribution by the remaining CDC potential in the mouse [3]. Lastly, CDC is known to be ineffective with tumor cells overexpressing complement resistance factors such as CD59 and CD55, which is frequently seen with tumor cell lines [5, 8]. This is especially true, as B16 cells could not be killed by in vitro CDC assays (data not shown).

In mouse models, monotherapy with humanized IgG1 antibodies rarely shows strong anti-tumor activity. While inhibition of tumor take or retardation of tumor outgrowth can be achieved, regression of established tumors is very difficult to observe. Certain monoclonal IgG1 antibodies are thought to have additional anti-tumor activity through inhibition of growth factor signaling or direct induction of apoptosis. Examples are anti-EGFR and anti-HER-2 antibodies [7, 16]. If their ADCC activity is suboptimal in mice due to a human Fc $\gamma$ 1 domain, the overall cytotoxic activity of such antibodies may be underestimated. At the same time, the contribution of signal inhibition to overall anti-tumor activity will be overrated. This has to be considered when judging the potential of a therapeutic antibody candidate. One possibility to achieve more reliable information about the effector mechanisms and potency of therapeutic antibody candidates would be to investigate analogous murine versions in mouse models. An alternative approach could be the development and use of genetic mouse models in which the genes encoding murine Fc $\gamma$ Rs are replaced by the respective human genes. Given there are three genes for Fc $\gamma$ Rs, generation of such knock-in/knock-out mice will be a major endeavor. The use of functionally equivalent murine Fc domains is much simpler and will moreover allow the use of different mouse strains and models. A yet different approach to assess contribution of immuno-



logical mechanisms to an antibody's cytotoxic activity is the use of F(ab)<sub>2</sub> fragments. In theory, F(ab)<sub>2</sub> fragments, which still bind target in a bivalent fashion, can inhibit tumor growth only by signaling effects but not through immunological effector mechanisms all of which are thought to reside in the Fc portion of the antibody.

Adecatumumab was shown to lyse tumor cells via ADCC and CDC, while no pro-apoptotic or anti-proliferative signaling activity has yet been demonstrated for this human antibody [11]. Adecatumumab was shown to significantly inhibit in nude mice for several weeks outgrowth of tumors derived from the subcutaneously inoculated human colon cancer cell line HT-29 [11]. Because HT-29 cells can be lysed by adecatumumab via ADCC, but not via CDC, only the former can account for anti-tumor activity in nude mice. Here, we found that human adecatumumab did not significantly reduce the number of lung metastases compared to an IgG1 isotype control in a syngeneic mouse model using B16/EpCAM melanoma cells but could substantially reduce the size of visible lung metastases. This shows that human adecatumumab clearly had anti-tumor activity in mice but was rather retarding tumor growth than preventing tumor formation, analogous to results from the HT-29 subcutaneous xenograft model [11]. In contrast, mu-adecatumumab showed a very pronounced inhibition of lung metastases formation. We therefore postulate that the in vivo anti-tumor activity of adecatumumab was thus far greatly underestimated in nude mouse models. The approach of exchanging human Fc $\gamma$ 1 with murine Fc $\gamma$ 2 taken here for adecatumumab should be applicable to all other human IgG1 therapies. In the case of antibodies with signaling activity, F(ab)<sub>2</sub> fragments should be tested in addition in mouse models.

How predictive is the efficacy seen with a mouse antibody in mice for an equivalent human antibody in humans? Certainly, fast-growing tumors established in mice from cell lines may only be distantly related to the natural, more slowly growing tumors in man, which display a higher degree of genetic heterogeneity of tumor cells, and may be different with respect to tissue morphology and stromal architecture. While issues of tumor penetration may be comparable in mouse and man, it may be harder for an antibody to control by ADCC a rapidly growing tumor in mice than a slowly growing tumor in man. Moreover, our present in vitro experiments indicate that murine immune cells are much less effective as human immune cells in ADCC, as they required for activity prolonged IL-2 stimulation, longer incubation periods and higher E:T ratios.

## References

1. Blumenthal RD, Osorio L, Hayes MK, Horak ID, Hansen HJ, Goldenberg DM (2005) Carcinoembryonic antigen antibody inhibits lung metastasis and augments chemotherapy in a human colonic carcinoma xenograft. *Cancer Immunol Immunother* 54:315–327
2. Cartron G, Dacheux L, Salles G, Solal-Celigny P, Bardos P, Colombat P, Watier H (2002) Therapeutic activity of humanized anti-CD20 monoclonal antibody and polymorphism in IgG Fc receptor Fc $\gamma$ RIIIa gene. *Blood* 99:754–758
3. Clynes RA, Towers TL, Presta LG, Ravetch JV (2000) Inhibitory Fc receptors modulate in vivo cytotoxicity against tumor targets. *Nat Med* 6:443–446
4. Dall'Ozzo S, Andres C, Bardos P, Watier H, Thibault G (2003) Rapid single-step FCGR3A genotyping based on SYBR Green I fluorescence in real-time multiplex allele-specific PCR. *J Immunol Methods* 277:185–192
5. Golay J, Zaffaroni L, Vaccari T, Lazzari M, Borleri GM, Bernasconi S, Tedesco F, Rambaldi A, Introna M (2000) Biologic response of B lymphoma cells to anti-CD20 monoclonal antibody rituximab in vitro: CD55 and CD59 regulate complement-mediated cell lysis. *Blood* 95:3900–3908
6. Golay J, Gramigna R, Facchinetti V, Capello D, Gaidano G, Introna M (2002) Acquired immunodeficiency syndrome-associated lymphomas are efficiently lysed through complement-dependent cytotoxicity and antibody-dependent cellular cytotoxicity by rituximab. *Br J Haematol* 119:923–929
7. Goldberg RM (2005) Cetuximab. *Nat Rev Drug Discov (Suppl.)*:S10–S11
8. Juhl H, Helmig F, Baltzer K, Kalthoff H, Henne-Bruns D, Kremer B (1997) Frequent expression of complement resistance factors CD46, CD55, and CD59 on gastrointestinal cancer cells limits the therapeutic potential of monoclonal antibody 17-1A. *J Surg Oncol* 64:222–230
9. Maloney DG, Smith B, Rose A (2002) Rituximab: mechanism of action and resistance. *Semin Oncol* 29:2–9
10. Mellstedt H (2003) Monoclonal antibodies in human cancer. *Drugs Today (Barc)* 39(Suppl. C):1–16
11. Naundorf S, Preithner S, Mayer P, Lippold S, Wolf A, Hanakam F, Fichtner I, Kufer P, Raum T, Riethmuller G, Baeuerle PA, Dreier T (2002) In vitro and in vivo activity of MT201, a fully human monoclonal antibody for pancreatic carcinoma treatment. *Int J Cancer* 100:101–110
12. Niwa R, Shoji-Hosaka E, Sakurada M, Shinkawa T, Uchida K, Nakamura K, Matsushima K, Ueda R, Hanai N, Shitara K (2004) Defucosylated chimeric anti-CC chemokine receptor 4 IgG1 with enhanced antibody-dependent cellular cytotoxicity shows potent therapeutic activity to T-cell leukemia and lymphoma. *Cancer Res* 64:2127–2133
13. Prang N, Preithner S, Brischwein K, Goster P, Woppel A, Muller J, Steiger C, Peters M, Baeuerle PA, da Silva AJ (2005) Cellular and complement-dependent cytotoxicity of Ep-CAM-specific monoclonal antibody MT201 against breast cancer cell lines. *Br J Cancer* 92:342–349
14. Preithner S, Elm S, Lippold S, Locher M, Wolf A, Silva AJ, Baeuerle PA, Prang NS (2006) High concentrations of therapeutic IgG1 antibodies are needed to compensate for inhibition of antibody-dependent cellular cytotoxicity by excess endogenous immunoglobulin G. *Mol Immunol* 43(8):1183–1193
15. Raum T, Gruber R, Riethmuller G, Kufer P (2001) Anti-self antibodies selected from a human IgD heavy chain repertoire: a novel approach to generate therapeutic human antibodies against tumor-associated differentiation antigens. *Cancer Immunol Immunother* 50:141–150

16. Sliwkowski MX, Lofgren JA, Lewis GD, Hotaling TE, Fendly BM, Fox JA (1999) Nonclinical studies addressing the mechanism of action of trastuzumab (Herceptin). *Semin Oncol* 26:60–70
17. Surfus JE, Hank JA, Oosterwijk E, Welt S, Lindstrom MJ, Albertini MR, Schiller JH, Sondel PM (1996) Anti-renal-cell carcinoma chimeric antibody G250 facilitates antibody-dependent cellular cytotoxicity with in vitro and in vivo interleukin-2-activated effectors. *J Immunother Emphasis Tumor Immunol* 19:184–191
18. Takai T (2002) Roles of Fc receptors in autoimmunity. *Nat Rev Immunol* 2:580–592
19. Weng WK, Levy R (2003) Two immunoglobulin G fragment C receptor polymorphisms independently predict response to rituximab in patients with follicular lymphoma. *J Clin Oncol* 21:3940–3947